Japanese Journal of Applied Physics
Vol. 47, No. 8, 2008, pp. 7005–7008

Sustainment of Plasma Density by a Low Magnetic Field in a Dual-Frequency Capacitively Coupled Plasma

Dae Ho KIM, Chang-Mo RYU, Sung Hee LEE[1], and Jae Koo LEE[1]

Department of Physics, Pohang University of Science and Technology, Pohang 790-784, Korea
[1]*Department of Electronic and Electrical Engineering, Pohang University of Science and Technology, Pohang 790-784, Korea*

(Received November 12, 2007; accepted February 1, 2008; published online August 22, 2008)

Dual-frequency capacitively coupled plasmas (DF-CCPs) have been used to control the ion flux by the high-frequency source and the ion bombardment energy onto the electrode by the low-frequency (LF) source separately. However, an increase in the LF voltage, which extends the maximum ion energy to a higher value, causes the reduction of the bulk plasma length with a subsequent decrease of the plasma density. By using a one-dimensional particle-in-cell/Monte Carlo simulation code, the effect of the magnetic field on a DF-CCP is investigated to find whether the plasma can be sustained during the LF voltage increase. It is found that a low magnetic field can effectively maintain the plasma density and electron temperature constant with respect to the variation of the LF voltage. [DOI: 10.1143/JJAP.47.7005]

KEYWORDS: capacitively coupled plasma, dual-frequency, magnetic field, particle-in-cell simulation

1. Introduction

Capacitively coupled radio-frequency (CCRF) discharges are widespreadly used in the micro-electronics industry for their applications such as thin-film deposition, etching, sputtering, and plasma cleaning.[1] As the semiconductor technology requires sub-micron processes, various kinds of CCRF sources have been developed to effectively improve the productivity of high-performance. In particular, dual-frequency capacitively coupled plasma (DF-CCP) devices developed by Goto *et al.*[2] have been of interest in their advantage of the high-frequency (HF) source to control the ion flux and the low-frequency (LF) source to control the ion bombardment energy independently onto the electrode. Therefore, much literature has been piled up on the use of DF-CCPs.[3–8] Using a one-dimensional particle-in-cell/Monte Carlo collision (1D PIC/MCC) simulation, Kim *et al.*[3] have developed a homogeneous plasma model for a DF-CCP which introduces the single effective frequency determined by the competition of two RF sources. Robiche *et al.*[4,5] have developed a model for a DF capacitive sheath with various gas pressures ranging from a few milliTorrs to hundreds of milliTorrs. In order to control the ion energy and ion flux more separately, Kitajima *et al.*[6] have observed experimentally in Ar/CF_4 discharges that the very high frequency of 100 MHz instead of 13.56 MHz is very useful for functional separation of LF biasing and HF sustaining voltages in a DF-CCP, with a fixed LF of 700 kHz. Georgieva *et al.*[7] also observed computationally that the dependence of the plasma density on the LF source is reduced in $Ar/CF_4/N_2$ discharges by increasing the applied HF to higher values (above 60 MHz).

Despite this feature, when the frequency of the HF source is below 60 MHz, an increase in the LF voltage, which extends the maximum ion energy to higher values, causes the reduction of the bulk plasma length with a subsequent decrease of the plasma density, because the ohmic heating power over the bulk plasma is reduced by the increasing LF voltage.[8] Hutchinson *et al.*[9] studied both experimentally and by using a 1D PIC/MCC simulation that the dominant electron heating mechanism in a low pressure discharge is changed from a stochastic sheath heating mode to a bulk ohmic electron heating mode in a low magnetic field. Rauf[10] observed that applying magnetic field to a DF-CCP tends to decrease the nonlinear interaction of two RF sources and to isolate two RF sources by the reduction of the electron mobility. Furthermore, compared with the unmagnetized discharge under the same conditions, the width of the ion-energy-distribution function, depending on the time-averaged sheath potential, is found to extend further in a magnetic field of a few tens of gauss.[11] In this respect, it can be easily guessed that the magnetic field may be useful for the DF-CCP to increase the ohmic heating power and to decrease the coupling of two RF sources in the bulk plasma.

In this paper, we investigate the application of the magnetic field to a DF-CCP for the purpose of maintaining the plasma density while the LF voltage increases, using a 1D PIC/MCC simulation. The simulation results show that compared to the unmagnetized discharge, even a low magnetic field can maintain the plasma density and electron temperature effectively during the LF voltage increase.

2. Simulation Conditions

The simulation has been carried out to study the low magnetic field effect on sustaining the plasma density under the increase of the LF voltage, by using a 1D PIC/MCC code (XPDC1).[12] Cylindrical geometry is chosen to simulate an asymmetric discharge with two electrodes of different sizes.[13] Two RF voltages at frequencies of 27 (HF) and 2 (LF) MHz are applied to the electrodes, while varying the LF voltage and fixing the HF voltage of 720 V. The area of the HF electrode is twice larger than that of the LF electrode and the gap distance is 2 cm. The secondary electron emission coefficient (SEEC: γ_{se}) for argon ion is taken to be 0. Argon gas is used at a pressure of 40 mTorr. A static magnetic field (B) of 30 G is applied parallel to the electrode surface. An additional set of simulation has been performed by using constant $B = 20$ G, SEEC $= 0.2$, HF voltage of 200 V and varying the LF voltage.

In the PIC simulation, we use about 300 superparticles per each grid and the time step of 2×10^{-12} s for the stability and accuracy of the simulation. The grid size is small enough to resolve the Debye length at the center of discharge. The time step is less than the minimal time

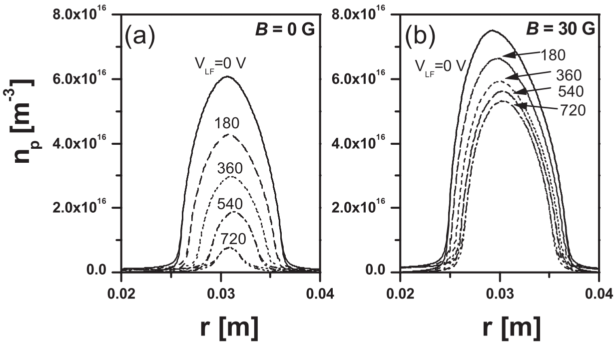

Fig. 1. Spatial profiles of the plasma density for various LF voltages (a) without and (b) with a magnetic field of 30 G at $p = 40$ mTorr and $V_{HF} = 720$ V.

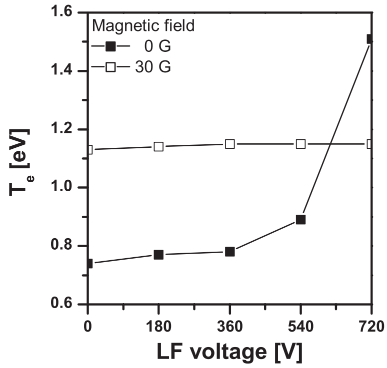

Fig. 2. Electron temperature at the discharge center as a function of the LF voltage without and with a magnetic field of 30 G at $p = 40$ mTorr and $V_{HF} = 720$ V.

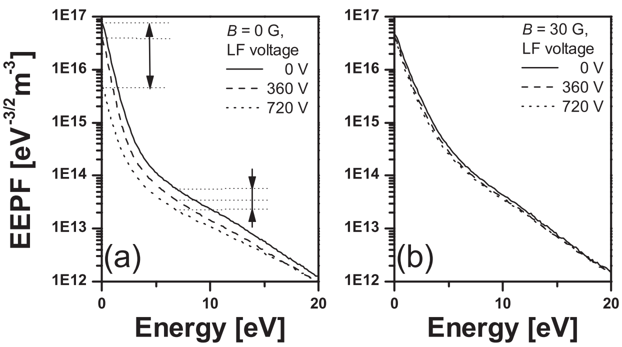

Fig. 3. Electron-energy-probability function at the discharge center for different LF voltages (a) without and (b) with a magnetic field 30 G at $p = 40$ mTorr and $V_{HF} = 720$ V.

scales in the discharge like the inverse electron plasma frequency and maximal collision frequency. The simulation is run for several hundreds of LF cycles until they reached the steady state.

3. Results and Discussion

Figure 1 depicts the spatial profiles of the plasma density for different LF voltages for the cases without a magnetic field and then with a magnetic field of 30 G, averaged over 4 LF cycles in the 27 and 2 MHz capacitive discharge at a pressure of 40 mTorr, when the HF voltage is kept at 720 V. In the absence of a magnetic field, an increase in the LF voltage decreases the plasma density from about 6.1×10^{16} to 7.9×10^{15} m^{-3} and the bulk plasma length from about 10 to 4 mm, as the LF voltage increases up to 720 V. Similar trends are reported in previous papers.[3–8)] It can be seen that the sheath width increases with an increasing LF voltage. The extension of the sheath width causes the impedance in the sheath to increase and the increase of the impedance results in the decrease of the conduction current. The reduction of the conduction current leads to the decrease of the ionization rate and the plasma density.

Next, the static magnetic field is applied parallel to the electrode surface and increases up to 30 G under the fixed HF and LF voltages of 720 V. It is observed that the plasma density increases sharply from 7.9×10^{15} to 5.3×10^{16} m^{-3}. As shown in Fig. 1(b), the decrement of the plasma density for the $B = 30$ G case is much less than those observed in the case of $B = 0$ G while the LF voltage increases up to 720 V. The bulk plasma length is slightly reduced from 11 to 7.9 mm in accordance with a decrease in plasma density. Therefore, a magnetic field seems to largely decrease the influence of the LF voltage on the reduction of the bulk plasma length.

The electron temperature (T_e) at the discharge center for different LF voltages without and with a magnetic field of 30 G is shown in Fig. 2. Whereas T_e for the $B = 30$ G case has approximately the same value with respect to the LF voltage, a rapid increase in T_e for the $B = 0$ G case is observed right beyond $V_{LF} = 540$ V.

The electron-energy-probability functions [EEPFs: $f_e(\epsilon)$] at the discharge center for various LF voltages without and with a magnetic field of 30 G are presented in Fig. 3 for examining the different behaviors of T_e. The EEPF is related to the electron-energy-distribution function [EEDF: $g_e(\varepsilon) = \varepsilon^{1/2} f_e(\varepsilon)$]. Without a LF voltage, the obtained EEPF shows a typical bi-Maxwellian distribution with two values of T_e ($T_{el} = 0.5$ eV and $T_{eh} = 3.7$ eV, where T_{el} and T_{eh} are low- and high-energy electron temperature, respectively). In low pressure argon RF discharges, the electrons can be divided into two groups of electrons associated with the moving high voltage sheath and ambipolar potential in the discharge center.[14,15)] One of those groups is the high-energy electrons, which overcome the ambipolar potential barrier and are stochastically heated by the moving high voltage sheaths. The other is the low-energy electrons with their low temperature, which are confined in the bulk by the ambipolar potential and thus unable to gain energy from the weak RF field in the bulk plasma (collisional heating). As a result, the overall electron energy distribution is described by bi-Maxwellian distributions.

When the LF voltage increases up to 720 V, two electron temperatures are insignificantly changed to $T_{el} = 0.5$ eV and $T_{eh} = 4.2$ eV. Hence, the population of the low-energy electrons originated from inelastic collisions considerably decreases by a factor of 8 while the bulk plasma length decreases with increasing LF voltage. In the case of a magnetic field of 30 G, the electron density slightly decreases with increasing LF voltage and two electron temperatures ($T_{el} = 0.8$ eV and $T_{eh} = 2.9$ eV) keep up the same values with an error of 0.05 eV. The trend for the $B = 30$ G case also shows the reduction of the LF influence by the magnetic field in the 27 and 2 MHz capacitive discharge. However, T_{el} changes from 0.5 to 0.8 eV, because

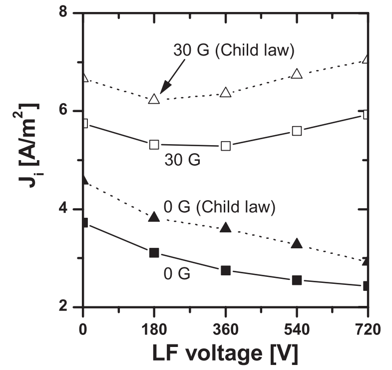

Fig. 4. Time-averaged ion current density at the LF electrode as a function of the LF voltage without and with a magnetic field of 30 G. The Child law of ion current density for the self-consistent RF ion sheath is chosen to compare with two different behaviors of ion current depending on the magnetic field at $p = 40$ mTorr and $V_{HF} = 720$ V.

the low-energy electrons just start to gain their energy by the magnetic field during electron-neutral collision processes.

The time-averaged ion current densities ($\bar{J}_i$) onto the LF electrode without and with a magnetic field (30 G) are plotted as a function of the LF voltage, which is shown in Fig. 4. In addition, the Child law of $\bar{J}_i$ for the self-consistent RF ion sheath is selected to compare with two different behaviors of $\bar{J}_i$ depending on the sheath potential and maximum sheath width. With a rise in the LF voltage, the behavior of $\bar{J}_i$ for $B = 0$ G is similar to the one of the plasma density. Since the ions are collisionless in the sheath, $\bar{J}_i$ onto the electrode is determined by the plasma density and electron temperature ($\bar{J}_i = n_{sh}e\sqrt{eT_e/M_i}$, where n_{sh} is the plasma density at the plasma edge, e is the elementary charge, and M_i is argon ion mass).[16] Thus, $\bar{J}_i$ for $B = 0$ G decreases continuously due to the reduction of the plasma density by increasing the LF voltage. Though the plasma density for $B = 30$ G decreases gradually with increasing LF voltage (see Fig. 1), $\bar{J}_i$ reduces a little but until the LF voltage reaches 360 V and then rises somewhat with an increasing LF voltage.

Considering the Child law of $\bar{J}_i$ for the self-consistent RF ion sheath in a parallel plate model,[16] $\bar{J}_i$ can be determined by

$$\bar{J}_i \approx 0.82\epsilon_0\left(\frac{2e}{M_i}\right)^{1/2}\frac{\bar{V}_{sh}^{3/2}}{s_m^2}, \qquad (1)$$

where ϵ_0, $\bar{V}_{sh}$, and s_m are the permittivity of free space, time averaged sheath potential and maximum sheath width in the LF sheath region, respectively. Though, the simulation has been carried out in an asymmetric geometry with a magnetic field, the Child law of $\bar{J}_i$ is enough to explain two different trends of $\bar{J}_i$ obtained from the simulation, because the ions are not magnetized between the two electrodes ($r_{ci} \sim 5$ cm > 2 cm,[16] where r_{ci} is the gyroradius for an argon ion). The calculated $\bar{J}_i$ attained from the simulation results of $\bar{V}_{sh}$ and s_m exhibits larger than the observed one. However, the calculated $\bar{J}_i$ for magnetic fields of 0 and 30 G shows a similar behavior as the one obtained for $\bar{J}_i$. An increase in the LF voltage for the $B = 0$ G case continues to increase the sheath potential to extend the sheath width until the discharge collapses. In the case for $B = 30$ G, while the sheath potential increases with a rising LF voltage, the extension of the sheath width by increasing the LF voltage is reduced much lower than the case for $B = 0$ G. The concave behavior of $\bar{J}_i$ is due to the competition of the sheath potential and the sheath width. Therefore, a low magnetic field in the 27 and 2 MHz capacitively coupled discharge largely decreases the influence of the LF voltage to broaden the sheath width. This result indicates the maintenance of the plasma density and electron temperature under the variation of the LF voltage.

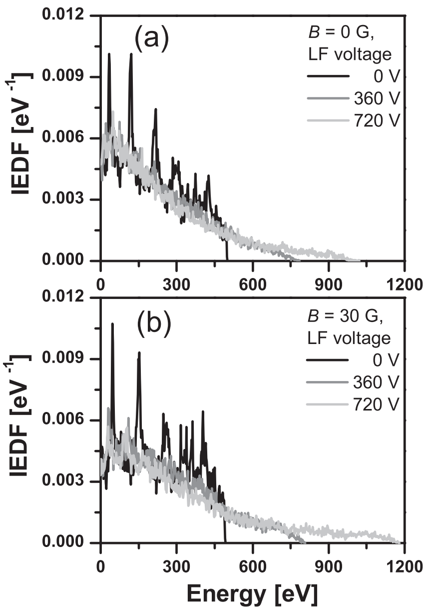

Fig. 5. Ion-energy-distribution functions for various LF voltages [0 (black line), 360 (gray line), and 720 V (light gray line)] and magnetic fields [(a) 0 and (b) 30 G] at $p = 40$ mTorr and $V_{HF} = 720$ V.

Figure 5 presents the ion-energy-distribution functions (IEDFs) at the LF electrode for various LF voltages (0, 360, and 720 V) and magnetic fields (0 and 30 G), averaged over 4 LF cycles in the 27 and 2 MHz capacitive discharge at a pressure of 40 mTorr. Without a LF voltage, the number of peaks and the maximum ion energy for $B = 0$ G show almost the same results as in the $B = 30$ G case. These peaks arise due to the acceleration of slow ions, which are created in the sheath as a result of charge-exchange collisions. The number of peaks (N) is determined by the driving frequency (f_{HF}), maximum sheath width, and the sheath potential ($N = 2f_{HF}s_m\sqrt{M_{Ar}/2e\bar{V}_{sh}}$).[17] From the simulation data, for $B = 0$ G, $\bar{V}_{sh} = 461$ V, $s_m = 0.0057$ mm and N is estimated to be about 6.5. For $B = 30$ G, $\bar{V}_{sh} = 445$ V, $s_m = 0.0046$ mm and N is calculated to be about 5.4. These values are in agreement with those observed in our simulation.

A rise in the LF voltage extends the maximum ion energy to higher values, which is one of the practical merits to use DF-CCPs for etching processes. While the LF voltage increases up to 720 V, the IEDFs for the $B = 30$ G case shows the same shapes as those for the $B = 0$ case, with a little exception for the position change of the maximum ion energy. When the LF voltage is kept at 720 V, the maximum ion energy for $B = 30$ G extends 16% higher than the case for $B = 0$ G, which seems to result from the enhancement of the negative dc-bias to about -60 V. Consequently, a low magnetic field does not affect much the shape of the IEDF at the LF electrode for the variation of the LF voltage.

As shown above, a low magnetic field case greatly reduces the influence of the LF voltage on the properties of

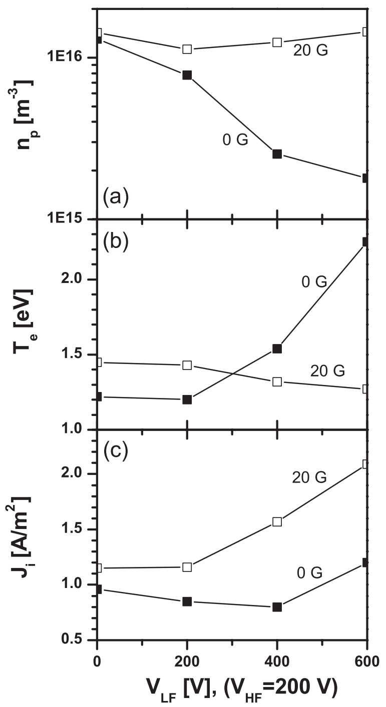

Fig. 6. (a) plasma density, (b) electron temperature in the discharge center, and (c) ion current density at the LF electrode, averaged over four LF cycles, as a function of the LF voltage without and with a magnetic field of 20 G at $p = 40$ mTorr and $V_{HF} = 200$ V.

discharge such as the plasma density, electron temperature, and ion current density. Further simulation was performed to confirm the trends of the plasma characteristics with the increase of the LF voltage at conditions of $\gamma_{se} = 0.2$ and $V_{HF} = 200$ V.

Figure 6 shows the simulation results for the plasma density, electron temperature in the discharge center, and ion current density at the LF electrode, as a function of LF voltage without and with a magnetic field of 20 G, averaged over 4 LF cycles in the 27 and 2 MHz capacitive discharge. Without a magnetic field, as the LF voltage increases up to 600 V, the plasma density decreases from about 1.3×10^{16} to 1.8×10^{15} m^{-3} and the bulk plasma size decreases from about 12 to 1.5 mm. The electron temperature shows the same value until a LF voltage value 200 V, and then increases with a higher LF voltage. However, the ion current density decreases slightly until the LF voltage reaches 400 V, and then increases further. These trends with the increase of the LF voltage are shown to be similar to those observed in the previous case of $\gamma_{se} = 0$.

When a magnetic field of 20 G is applied to the 27 and 2 MHz capacitive discharge, it is observed that the plasma density is sustained almost at the same value for an increasing LF voltage. The electron temperature slightly decreases from about 1.5 to 1.3 eV. The ion current density increases linearly above 200 V of the LF voltage. A slight different behavior in the plasma density between $\gamma_{se} = 0$ ($B = 30$ G) and 0.2 ($B = 20$ G) cases is observed, while the LF voltage increases. It would be due to the fact that the magnetized secondary electrons partially correspond to ionize neutrals in the bulk plasma. For example, a magnetic field of 20 G can confine some secondary electrons to dissipate their energy within the 2 cm gap length, because the gyroradius for a 130 eV electron is 1.9 cm. Thus, the ionization by the secondary electrons increases the plasma density gradually above 200 V of the LF voltages.

4. Conclusions

Dual-frequency capacitively coupled plasmas are in general used to control the ion flux by the high-frequency source and the ion bombardment energy onto the electrode by the low-frequency source independently. However, the increase of the low-frequency voltage leads to the reduction of the bulk plasma length with a subsequent decrease of the plasma density.

To investigate the effect of the magnetic field on a dual-frequency capacitively coupled plasma for the maintenance of the plasma density, a one-dimensional particle-in-cell/Monte Carlo collision simulation code has been used. The simulation results show that a low magnetic field in a 27 and 2 MHz capacitively coupled discharge largely reduces the sheath width for the increased the LF voltage, resulting that the magnetic field can sustain the plasma density and electron temperature constantly during the LF voltage variation. Compared to the unmagnetized discharge, it is found that a low magnetic field does not affect much the shape of the ion-energy-distribution function at the low-frequency electrode during the variation of the low-frequency voltage. It is found also that whereas the plasma density decreases continuously for the $\gamma_{se} = 0$ case when the low-frequency voltage increases, the plasma density for the $\gamma_{se} = 0.2$ case slightly increases due to the ionization of the magnetized secondary electrons.

Acknowledgment

This research was supported by the Program for the Training of Graduate Students in Regional Innovation which was conducted by the Ministry of Commerce Industry and Energy of the Korea Government.

1) J. R. Roth: *Industrial Plasma Engineering* (IOP Publishing, Bristol, U.K., 1995) Chap. 12.
2) H. H. Goto, H.-D. Löwe, and T. Ohmi: J. Vac. Sci. Technol. A **10** (1992) 3048.
3) H. C. Kim, J. K. Lee, and J. W. Shon: Phys. Plasmas **10** (2003) 4545.
4) J. Robiche, P. C. Boyle, M. M. Turner, and A. R. Ellingboe: J. Phys. D **36** (2003) 1810.
5) P. C. Boyle, J. Robiche, and M. M. Turner: J. Phys. D **37** (2004) 1451.
6) T. Kitajima, Y. Takeo, Z. Lj. Petrovic, and T. Makabe: Appl. Phys. Lett. **77** (2000) 489.
7) V. Georgieva and A. Bogaerts: J. Appl. Phys. **98** (2005) 023308.
8) T. H. Chung: Phys. Plasmas **12** (2005) 104503.
9) D. A. W. Hutchinson, M. M. Turner, R. A. Doyle, and M. B. Hopkins: IEEE Trans. Plasma Sci. **23** (1995) 636.
10) S. Rauf: IEEE. Trans. Plasma Sci. **31** (2003) 471.
11) D. Kim, H. Chang, and C.-M. Ryu: Comput. Phys. Commun. **177** (2007) 125.
12) C. K. Birdsall: IEEE Trans. Plasma Sci. **19** (1991) 65.
13) J. K. Lee, N. Yu. Babaeva, H. C. Kim, O. V. Manuilenko, and J. W. Shon: IEEE Trans. Plasma Sci. **32** (2004) 47.
14) V. A. Godyak and R. B. Piejak: Phys. Rev. Lett. **65** (1990) 996.
15) I. D. Kaganovich and L. D. Tsendin: IEEE Trans. Plasma Sci. **20** (1992) 66.
16) M. A. Lieberman and A. J. Lichtenberg: *Principles of Plasma Discharges and Materials Processing* (Wiley, New York, 1994) Chap. 11.
17) J. C. Park and B. Kang: IEEE Trans. Plasma Sci. **25** (1997) 499.